338
GEOME 2
Manuscript received: August 5, 2018
Accepted: November 7, 2018

Geologica Macedonica, Vol. **32**, No. 2, pp. 95–117 (2018)
IISSN 0352 – 1206
e-ISSN 1857 – 8586
UDC: 553.46:550.43.08]:504(497.721)
553.497:550.43.08]:504(497.721)

Original scientific paper

SUPERGENE MINERALOGY OF THE LOJANE Sb-As-Cr DEPOSIT, REPUBLIC OF MACEDONIA: TRACING THE MOBILIZATION OF TOXIC METALS

Uwe Kolitsch[1,2], Tamara Đorđević[2], Goran Tasev[3], Todor Serafimovski[3], Ivan Boev[3], Blažo Boev[3]

[1]*Mineralogisch-Petrographische Abt., Naturhistorisches Museum, Burgring 7, A-1010 Wien, Austria*
[2]*Institut für Mineralogie und Kristallographie, Universität Wien, Althanstr. 14, A-1090 Wien, Austria*
[3]*Department of Mineral Deposits, Faculty of Natural and Technical Sciences, "Goce Delčev" University in Štip, Blvd. Goce Delčev 89, 2000 Štip, Republic of Macedonia*
uwe.kolitsch@nhm-wien.ac.at

A b s t r a c t: As part of a larger project on the environmental mineralogy and geochemistry of the Lojane Sb-As-Cr deposit, Republic of Macedonia, which was mined for chromite and, later, stibnite until 1979 and is a substantial source of arsenic and antimony pollution, the supergene mineralogy of the deposit was studied. Samples collected on ore and waste dumps were used to identify and characterize the previously uninvestigated suite of supergene mineral phases by standard mineralogical techniques. The following species were determined (in alphabetical order): annabergite, arseniosiderite(?), gypsum, hexahydrite, hörnesite, pararealgar, roméite-group minerals, rozenite, scorodite, senarmontite, stibiconite, sulphur, tripuhyite and valentinite. Their occurrences are described and their local conditions of formation are discussed. High-resolution Raman spectra of hörnesite, hexahydrite and rozenite are provided and compared with literature data. The Mg arsenate hörnesite is by far the most common secondary arsenate (and immobilizer of arsenic), an observation attributed to the Mg- and carbonate-rich serpentinite matrix which buffers any acid weathering solutions. Antimony is efficiently immobilized in secondary Sb(III) oxides, but trace amounts are also incorporated into scorodite. Nickel, derived from primary Ni(-bearing) sulphide and sulpharsenide minerals, is mobilized and incorporated into annabergite and chemically variable roméite-group minerals. No mobilization of Cr was noted, in agreement with literature data on weathered Cr deposits.

Key words: Lojane deposit; Republic of Macedonia; supergene mineralogy; arsenic; antimony; chromium

INTRODUCTION

The Lojane Sb-As-Cr deposit is located in the north-eastern part of the Republic of Macedonia, about 2 km SW of the village of Lojane and about 10 km NNW of the city of Kumanovo (for details see section "Geology"). The deposit was mined for chromite and stibnite from 1923–1979 (Stuhlberger, 2010). The various mine dumps and the tailings dump present one of the major environmental problems for Macedonia and are considered a very serious human health risk given high concentration of arsenic- and antimony-rich wastes (Alderton et al., 2014, and references therein). The orange tailings dump (42.217303 N, 21.664378 E), about 30 × 50 m in size and located immediately adjacent to the dilapidated processing plant, is not covered and represents a substantial source of arsenic and antimony pollution. This tailings dump consists of a fine-grained mixture of major realgar, pararealgar, gypsum, stibnite and minor amounts of quartz, carbonates and various other primary and secondary phases (e.g. scorodite, roméite-group minerals, several sulphates) in minor to trace amounts (Đorđević et al., 2018b).

Remediation of the former Lojane mine site has not proceeded despite United Nations Environment Programme (UNEP) and United Nations Development Programme (UNDP) initiatives in the mid-2000s (UNEP, 2000; JICA et al., 2008; Williams & Marstijepovic, 2010).

The Lojane area, at an altitude of about 440 to 640 m, is characterized by a mild, generally warm and temperate mediterranean climate. The average annual temperature is 11.2 °C and the average rainfall is 544 mm. There is a significant amount of rainfall during the year, even in the driest month.

We have started to study, in detail, the environmental mineralogy and geochemistry of the Lojane Sb-As-Cr deposit in a 4-year research project (1/2018–12/2021), which was preceded by a smaller reconnaissance research project (5/2016–

6/2018) that focused on the deposit's weathering products occurring on ore, waste and tailings dumps.

The broad aims of our comprehensive study are as follows:

(i) Re-study the primary mineralogy in detail (the most recent prior studies of the Sb-As mineralization date back to the 1960s).

(ii) Characterize the previously uninvestigated supergene mineralogy of the deposit and its waste material, including poorly crystalline and amorphous secondary phases.

(iii) Search for the host mineral(s) of the Ni reported in a geochemical study of the ore (Ni 10–50 ppm; Janković, 1989).

(iv) Search especially for any primary or secondary thallium minerals, since Janković (1989) reported increased Tl content of the realgar from Lojane (100–1000 ppm).

(v) Conduct a detailed geochemical study of pore water.

(vi) Quantify the distribution of contaminants (As, Sb, Tl, Cr) in the waste dumps, and evaluate the geochemical controls on dissolved As, Sb, Tl and Cr.

The first results from our studies were presented in three conference abstracts (Đorđević et al., 2017, 2018; Tasev et al., 2017).

The present contribution, one of the various results of the reconnaissance project, gives details on the supergene mineralogy of the Lojane deposit. It also discusses the conditions of formation of the observed secondary phases and it provides a discussion of the implications for the mobilization of the environmentally hazardous elements As, Sb, Cr and Ni. The primary mineralogy is still under investigation and results will be presented in a future paper. Furthermore, we present high-resolution laser-Raman spectra of hörnesite, hexahydrite and rozenite and compare them with literature data.

GEOLOGY AND ORE MINERALOGY

The Lojane area features a unique ore-deposit geology. In brief, fault-bound vein-type low-temperature realgar-stibnite mineralization (in part with dolomite and calcite gangue) is located at the contact between a rhyolite of Miocene-Pliocene age (Karamata, 1983; Mudrinić, 1978; Serafimovski, 1990, 1993; "andesite" of the older literature) and an older (Jurassic-Cretaceous) ophiolitic, silicified serpentinite containing podiform chromite bodies. Locally, the mineralization is also hosted by the serpentinite itself and in the immediate vicinity of chromite bodies or within the latter (Janković, 1960). Young (Cretaceous) granite intrusions and granodioritic dykes (whole-rock K-Ar age: 92 Ma; Serafimovski, 1990) also occur in the area. Geologically, the mineralized area is located in the NW-SE to N-S striking Vardar zone (also called Sava-Vardar zone), a very heterogeneous lithological domain, which, among other units, contains the suture zone that developed during the collision between Eurasia and Adria at the end of the Cretaceous (Pamić, 2002).

A detailed and excellent account of the geology of the area and the As-Sb-Cr mineralization is given by Hiessleitner (1931, 1934), results of which were later summarized in Hiessleitner (1951) and updated in Schumacher (1954). Subsequently, Antonović et al. (1957) and Deleon (1959) reported results from investigations of the As-Sb ore. Fairly detailed descriptions of both geology and As-Sb ore mineralization are given by Janković (1960) and Radusinović (1966). A comprehensive study on geology, tectonic structure and genesis of the As-Sb deposit was published by Antonović et al. (1965), who provided many macroscopic and reflected-light microscopic photographs of ore textures (e.g. dolomite veins with realgar, breccias, microbreccias, collomorphic ore types, stibnite oolites, stibnite replaced by realgar). The only further studies were published by Grafenauer (1977), who focused on the chromite deposit, and Augé et al. (2017), who reported some platinum-group minerals detected in the ophiolite-hosted chromite ore.

Our recent studies of both the realgar-stibnite ore and the chromite ore by modern mineralogical methods revealed a larger number of previously undetected sulphide and arsenide phases (Đorđević et al., 2017), including several primary Ni(-As) minerals (see Table 1 further below). The most widespread Ni mineral is gersdorffite that forms rounded, commonly finely zoned (concentric or patchy) aggregates up to 20 μm, which occur in realgar, stibnite and quartz. Nearly all of the observed sulphides (pyrite, vaesite, minor pyrrhotite, rare thiospinels) often contain trace to minor amounts of As, reflecting the As-rich environment. Some As- and Ni-bearing pyrite also contains trace amounts of Sb. Ongoing studies of chromite ore specimens led to the detection of very rare laurite (RuS_2), independently also confirmed by Augé et al. (2017).

SAMPLING

Samples were collected in November 2016, May 2017 and May 2018 from several ore and waste dumps along the western and (mainly) eastern slopes of the valley cutting the mineralization, but mainly from a large, elongate ore-rich dump (42.214933 N, 21.654994 E; Figures 1–2), which seems to represent a temporary storage site of mined material scheduled to be transported to the nearby processing plant (42.218060 N, 21.664580 E). The dump shows a maximum height of about 2–3 m. It is located immediately adjacent to the valley's creek bed about 3–4 m lower, and, as visible in Figure 3, dump material erodes into the creek during the wet period (in the summer season the creek falls dry).

Fig. 1. Large, elongate ore-rich dump cut by a trench, approximately 1.5 m in depth, which was excavated in 2017 by a Turkish exploration company. This trench facilitated sampling and observation of supergene phases. Photo T. Đ. in April 2018.

Fig. 2. Large realgar-stibnite ore boulder on the largest dump. Photo T. Đ. in April 2018

Fig. 3. Large ore-rich dump (left) whose western flank is eroded by the intermittently water-bearing small creek (right), Photo T. Đ. in April 2018

In July–August 2017, a Turkish exploration company had dug a trench, approximately 1.5 m in depth, along the major axis of the mentioned ore-rich dump (Figure 1). This trench strongly facilitated the observation of weathering processes inside the dump and the sampling of suitable material from different depths. It is well known that weathering conditions of As-rich mining waste within a dump can range from oxidizing to reducing, and can vary with groundwater level and microclimate, leading to microenvironments of mineral species stable under different conditions (DeSisto et al., 2016). The dump appeared fairly well aerated down to the lower trench level. On nearly vertical parts of the trench walls, white, recent efflorescences of a crumbly nature and dull appearance were also sampled.

An adit (approx. 42.215010 N, 21.653290 E) on the southwestern slope of the valley is flooded starting at a distance about 10 m from the entrance. No secondary phases were observed on the walls of the accessible part of this adit.

EXPERIMENTAL METHODS

The supergene mineral phases were studied by a combination of standard mineralogical techniques best suited for the purpose of the present study. We employed optical microscopy, single-crystal and powder X-ray diffraction (SXRD and PXRD, respectively), Raman spectroscopy and SEM-EDS analyses. For the SXRD investigations, a Nonius KappaCCD single-crystal diffractometer (Mo$K\alpha$ radiation) equipped with a CCD area detector was used. For the PXRD studies, we employed the same diffractometer that is able to record, in a Gandolfi-like technique, digital powder patterns. The Raman spectra were measured with a Horiba-Yvon LabRAM HR confocal laser micro-Raman spectrometer, equipped with an Olympus BX41 optical microscope, in the spectral range from 100 to 4000 cm^{-1}. The 632.8 nm excitation line of a He–Ne laser was focused with a 50× objective (N.A. = 0.90) on randomly oriented single crystals. The spectra were acquired with a nominal exposure time of maximal 60 s (confocal mode, 180° backscatter geometry, 1800 lines/mm, 1.5 μm lateral resolution, and approximately 3 μm depth resolution). For the SEM-EDS studies, we used a JEOL JSM-6610LV scanning electron microscope (at the Natural History Museum, Vienna, Austria) equipped with a high-

sensitivity and high-resolution energy-dispersive X-ray spectrometer (Bruker e-FlashHR+; detector area 30 mm^2, resolution 127 eV) and Bruker Esprit 2.0 software (which applies spectrum deconvolution). The accuracy of the standardless analyses (15 kV, 60 s measuring time, spatial resolution 0.1–1 micron, PB-ZAF correction) is estimated to be 2–3% for "common" minerals and better than 5–10% for "uncommon" minerals with unusual chemical compositions, based on six-year experience of studying a large variety of polished mineral, ore and rock samples. In case of strong peak overlaps, when errors may exceed 10%, analytical results were compared to those of external standards. In some cases, ore microscopical studies were performed to supplement the SEM-EDS investigations.

Single crystals or single-phase crystal aggregates and crusts of the supergene phases were selected under an optical microscope and fragments thereof were mechanically removed from the samples. Both fresh and weathered ore samples were studied using polished and carbon-coated aliquots embedded in resin (standard one-inch-diameter cylinders). Presently, a total of 24 polished sections were studied.

SUPERGENE MINERALOGY

In the following paragraphs, we describe the detected supergene minerals and their occurrences. All primary and secondary mineral species presently known from Lojane are listed in Tables 1 and 2, respectively, along with the method(s) used to identify them. Selected Raman spectra are given and discussed in a subsequent section.

T a b l e 1

Primary and secondary mineral species presently known from the Lojane Sb-As-Cr deposit, Republic of Macedonia, each in alphabetical order.Methods of identification are given as superscripts (see table footnote)

Primary phases	Chemical formula	Reference(s)
a) Sulphides, sulpharsenides, arsenides and antimonides		
Arsenic (or arsenolamprite?)[4]	As	Đorđević et al. (2017)
Cattierite	CoS_2	Janković (1960)
Chalcopyrite[4]	$CuFeS_2$	Đorđević et al. (2017)
Duranusite[4]	As_4S	Đorđević et al. (2017)
Galena[4]	PbS	Đorđević et al. (2017)
Gersdorffite[4]	NiAsS	Đorđević et al. (2017)
Greigite	$Fe^{2+}Fe^{3+}{}_2S_4$	Radusinović (1966)
Kermesite	Sb_2S_2O	Antonović et al. (1965)
Laurite[4]	RuS_2	Augé et al. (2017), Đorđević et al. (2017)
Marcasite	FeS_2	Antonović et al. (1957), Janković (1960), Radusinović (1966)
Millerite[4]	NiS	Đorđević et al. (2017)
Naldrettite(?)[4]	Pd_2Sb	Đorđević et al. (2017)
Orpiment[4]	As_2S_3	Hiessleitner (1934), Deleon (1959), Janković (1960), Radusinović (1966), Đorđević et al. (2017)
Parkerite(?)[4]	$Ni_3Bi_2S_2$	Đorđević et al. (2017)
Pentlandite[4]	$(Fe_xNi_y)_{\Sigma 9}S_8$, where $x+y=9$	Đorđević et al. (2017)
Polydymite[4]	$Ni^{2+}Ni^{3+}{}_2S_4$	This work, Đorđević et al. (in prep.)

Primary phases	Chemical formula	Reference(s)
Pyrite[4] (often As-bearing)	FeS_2	Hiessleitner (1934), Antonović et al. (1957), Janković (1960), Antonović et al. (1965), Radusinović (1966), Đorđević et al. (2017)
Pyrite ("bravoite")	$(Fe,Ni)S_2$	Antonović et al. (1957), Vujanović (1958), Janković (1960), Antonović et al. (1965), Radusinović (1966)
Pyrrhotite[4]	Fe_7S_8	Đorđević et al. (2017)
Realgar[3, 4]	AsS	Hiessleitner (1934, 1951), Antonović et al. (1957), Janković (1960), Antonović et al. (1965), Radusinović (1966), Đorđević et al. (2017)
Sphalerite[4]	ZnS	Đorđević et al. (2017)
Stibnite[3, 4)]	Sb_2S_3	Hiessleitner (1934), Antonović et al. (1957), Deleon (1959), Janković (1960),Antonović et al. (1965), Radusinović (1966), Đorđević et al. (2017)
Ullmannite[4]	NiSbS	Đorđević et al. (2017)
Vaesite[4]	NiS_2	Antonović et al. (1957), Janković (1960), Radusinović (1966), Đorđević et al. (2017)
Violarite[4]	$Fe^{2+}Ni^{3+}{}_2S_4$	Đorđević et al. (2017)
b) Other phases		
Actinolite ("smaragdite")	$Ca_2(Mg,Fe^{2+},Cr)_5Si_8O_{22}(OH)_2$	Hiessleitner (1934)
Albite[4]	$NaAlSi_3O_8$	Đorđević et al. (2018b, in prep.)
Anatase	TiO_2	Đorđević et al. (2018b)
"Apatite"	$Ca_5(PO_4)_3(F,OH,Cl)$	Tajder (1939)
"Asbestos"		Hiessleitner (1934), Tajder (1939)
Baryte[4]	$BaSO_4$	Đorđević et al. (2017)
"Biotite"		Hiessleitner (1931)
Brucite	$Mg(OH)_2$	Tajder (1938)
Calcite	$CaCO_3$	Hiessleitner (1931, 1934)
Chromite[4]	$FeCr_2O_4$	Hiessleitner (1931, 1934), Janković (1960), Radusinović (1966), Grafenauer (1977), this work
Clinochlore	$Mg_5Al(AlSi_3O_{10})(OH)_8$	Schumacher (1954)
Clinochlore, Cr-bearing ("Kämmererite")	$Mg_5(Al,Cr)(AlSi_3O_{10})(OH)_8$	Hiessleitner (1931, 1934); Schumacher (1954)
Coffinite[4]	$U(SiO_4)\cdot nH_2O$	Đorđević et al. (2017)
Diopside[4] (incl. Cr-bearing variety)	$CaMgSi_2O_6$	Hiessleitner (1931, 1934), this work
Dolomite[4]	$CaMg(CO_3)_2$	Hiessleitner (1934), Janković (1960), Antonović et al. (1965), Radusinović (1966), this work
Epidote[4]	$\{Ca_2\}\{Al_2Fe^{3+}\}(Si_2O_7)(SiO_4)O(OH)$	Đorđević et al. (in prep.)
Eulytine[4]	$Bi_4(SiO_4)_3$	Đorđević et al. (in prep.)
Fluorapatite[4]	$Ca_5(PO_4)_3F$	Đorđević et al. (2018a)
"Garnet"		Hiessleitner (1934)

Primary phases	Chemical formula	Reference(s)
Hercynite[4]	$Fe^{2+}Al_2O_4$	This work, Đorđević et al. (in prep.)
"Hornblende"		Tajder (1939)
Hydroxylapatite[4]	$Ca_5(PO_4)_3(OH)$	Đorđević et al. (2017)
Kaolinite–illite[4]	$Al_3Si_2O_5(OH)_4$–$K_{0.65}Al_{2.0}[Al_{0.65}Si_{3.35}O_{10}](OH)_2$	Đorđević et al. (2017)
Magnesiochromite[4]	$MgCr_2O_4$	Đorđević et al. (2018a,b)
Magnesite[4]	$MgCO_3$	Hiessleitner (1931), Đorđević et al. (in prep.)
Magnetite[4]	$Fe^{2+}Fe^{3+}{}_2O_4$	Hiessleitner (1934), Radusinović (1966), Grafenauer (1977), Đorđević et al. (in prep.)
Maucherite(?)[4)]	$Ni_{11}As_8$	Đorđević et al. (2017)
Monazite-(Ce)[4]	$Ce(PO_4)$	This work, Đorđević et al. (in prep.)
Montmorillonite	$(Na,Ca)_{0.33}(Al,Mg)_2(Si_4O_{10})(OH)_2 \cdot nH_2O$	Radusinović (1966)
Muscovite[4]	$KAl_2(AlSi_3O_{10})(OH)_2$	Hiessleitner (1931), Đorđević et al. (2018a)
Opal	$SiO_2 \cdot nH_2O$	Hiessleitner (1931)
Phlogopite	$KMg_3(AlSi_3O_{10})(OH)_2$	Tajder (1939)
Quartz (incl.chalcedony)	SiO_2	Janković (1960), Antonović et al. (1965), Radusinović (1966), Đorđević et al. (2017)
Rutile[4]	TiO_2	Đorđević et al. (2018a)
Sepiolite group		Hiessleitner (1934)
"Serpentine"	$Mg_3(Si_2O_5)(OH)_4$	Hiessleitner (1931, 1934)
Siderite[4]	$FeCO_3$	Đorđević et al. (2017)
Spessartine[$]	$Mn_3Al_2(SiO_4)_3$	Jovanovski et al. (2012)
Spinel[4]	$MgAl_2O_4$	Đorđević et al. (in prep.)
Talc	$Mg_3Si_4O_{10}(OH)_2$	Hiessleitner (1934)
"Tourmaline"		Hiessleitner (1934)
Tremolite[4]	$\{Ca_2\}\{Mg_5\}(Si_8O_{22})(OH)_2$	Hiessleitner (1934), Đorđević et al. (in prep.)
Uraninite[4]	UO_2	Đorđević et al. (2017)
Uraninite ("Pitchblende")	UO_2	Janković (1960)
Uvarovite[4]	$Ca_3Cr_2(SiO_4)_3$	Hiessleitner (1934), Đorđević et al. (2017)
Zircon[4]	$ZrSiO_4$	Tajder (1939), Đorđević et al. (2017)
Unnamed Bi-As-S-Cl(-O?) phase[4]	Bi-As-S-Cl(-O?)	Đorđević et al. (2017), Đorđević et al. (in prep.)

[3)] Raman, [4)] SEM-EDS

[$)] Spessartine was reported by Jovanovski et al. (2012) on the basis of PXRD, and Raman spectra, but the occurrence of a Mn garnet is considered somewhat questionable here because it would be very unusual considering the geology of the deposit.

Note: From the general area of Lojane, vesuvianite and "apophyllite" were reported (Meixner, 1949), as well as the new mineral magnesiovesuvianite (Panikorovskii et al., 2017) which occurs in cavities of a garnet-bearing rodingite from the apocryphal locality "Tuydo combe"; accompanying minerals are andradite-grossular, calcite and clinochlore.

T a b l e 2

Secondary mineral species presently known from the Lojane Sb-As-Cr deposit, Republic of Macedonia, each in alphabetical order. Methods of identification are given as superscripts (see table footnote)

Secondary phases	Chemical formula	Reference(s)
Alunogen[3, 4, §§]	$Al_2(SO_4)_3 \cdot 17H_2O$	Đorđević et al. (2018b)
Annabergite[4]	$Ni_3(AsO_4)_2 \cdot 8H_2O$	Đorđević et al. (2017, 2018a), this work
Aragonite[1]	$CaCO_3$	Hiessleitner (1931, 1934), this work
Arseniosiderite(?)[4]	$Ca_2Fe^{3+}_3(AsO_4)_3O_2 \cdot 3H_2O$	Đorđević et al. (2017)
Arsenolite[3, 4, §§]	As_2O_3	Đorđević et al. (2018b)
Artinite	$Mg_2(CO_3)(OH)_2 \cdot 3H_2O$	Palache et al. (1951)
Goethite	FeO(OH)	Grafenauer (1977)
Gypsum[3, 4]	$CaSO_4 \cdot 2H_2O$	Đorđević et al. (2017), this work
Hexahydrite[2, 3]	$MgSO_4 \cdot 6H_2O$	This work
Hörnesite[2, 3]	$Mg_3(AsO_4)_2 \cdot 8H_2O$	Đorđević et al. (2017), this work
Hydromagnesite[2]	$Mg_5(CO_3)_4(OH)_2 \cdot 4H_2O$	Hiessleitner (1931, 1934), this work
Kaňkite(?)[3, §§]	$FeAsO_4 \cdot 3.5H_2O$	Đorđević et al. (2018a)
"Limonite"[4]	$Fe(O,OH,H_2O)$	This work, Đorđević et al. (2018b)
Pararealgar[3]	AsS	This work, Đorđević et al. (2018b)
Pickeringite[§§] (Fe^{2+}- and Ni^{2+}- bearing)	$MgAl_2(SO_4)_4 \cdot 22H_2O$	Đorđević et al. (2018b)
~~Picropharmacolite~~[§]	$Ca_4Mg(AsO_4)_2(HAsO_4)_2 \cdot 11H_2O$	Đorđević et al. (2017), this work
Roméite-group minerals[4]	$\sim(Ca,Fe,Ni)_2(Sb,As)^{5+}_2O_7$	Đorđević et al. (2017, 2018a), this work
Rozenite[2, 3]	$FeSO_4 \cdot 4H_2O$	This work
Scorodite[2,3]	$FeAsO_4 \cdot 2H_2O$	Đorđević et al. (2017, 2018a,b), this work
Senarmontite[1]	Sb_2O_3	Đorđević et al. (2017), this work
Sulphur[1]	α-S	Đorđević et al. (2018a), this work
"Stibiconite"[2]	$Sb^{3+}Sb^{5+}_2O_6(OH)$	This work
Tripuhyite(?)[4]	$Fe^{3+}Sb^{5+}O_4$	This work
Valentinite[1, 4]	Sb_2O_3	Đorđević et al. (2017), this work
Unidentified sulphate-arsenate(s)[4)§§]	Fe?-AsO_4-SO_4-H_2O	This work, Đorđević et al. (2018b)

[1)] SXRD, [2)] PXRD, [3)] Raman, [4)] SEM-EDS

[$] Picropharmacolite was erroneously reported by Đorđević et al. (2017); it was later recognized as hörnesite (see text for details)

[§§] Weathering product of tailings dump only.

Elements and sulphides

Sulphur is a very rare oxidation product of stibnite. On strongly weathered stibnite specimens, it forms tiny, pale yellow, blocky to rounded crystals. Nearby, crystals of valentinite and senarmontite were observed. Arsenic-bearing sulphur was also detected as a minor phase in the tailings (Đorđević et al., 2018a,b). Pararealgar (AsS) represents the only secondary sulphide observed so far. It forms as a typical light-induced isochemical alteration product of realgar (AsS) and is easily recognisable as orange, thin and fine-grained coatings on any realgar lying unprotected on dumps (Figure 4).

Fig. 4. Orange pararealgar (formed as a light-induced isochemical alteration product of realgar), with included dendritic stibnite. This specimen was found on the largest dump. Photo T. Đ. in May 2017.

The conspicuous orange colour of the tailings dump is due to a mixture of fine-grained pararealgar and realgar (Đorđević et al., 2018b). On the surface of the ore dumps, no secondary arsenate phases form on the pararealgar/realgar. Instead, the fine-grained and often crumbly pararealgar is seemingly subjected to mechanical weathering by rain and wind. Thus, although in the As–O–H system arsenic is fairly mobile under oxidizing and mildly reducing conditions (Lu & Zhu, 2011), secondary arsenates only form within the dump in colder and wetter conditions.

We note that the oxosulphide kermesite (Sb_2S_2O), reported by Antonović et al. (1965), may be considered a primary ore phase. We were unable to confirm the presence of kermesite so far.

Oxides and hydroxides

On several samples of partly to strongly weathered stibnite, secondary antimony oxides were identified, which are typical weathering products of stibnite and Sb-bearing ore minerals (Roper et al., 2012). Senarmontite forms tiny pale grey-pink or colourless to whitish octahedra (Figure 5).

Fig. 5. Colour photo of senarmontite forming tiny pale grey-pink octahedra (mainly in centre), in association with crude subparallel lath-shaped valentinite crystals (left), fresh stibnite (bottom and top right) and minor realgar (bottom left). Field of view 1.6 mm. Collection Natural History Museum Vienna. Photo Harald Schillhammer.

It is associated with valentinite that occurs as small, white to cream-coloured, prismatic, mostly incomplete crystals recognizable by a good cleavage and a strong greasy lustre. SEM-EDS analyses show trace amounts of As and Si as impurity elements. The presence of these Si traces is surprising. On another specimen, valentinite is associated with stibiconite and forms small pale grey to pale brown -grey, stubby to prismatic crystals with a faint striation parallel to their elongation. Both senarmontite and valentinite occupy a very large stability field, under moderately reducing to moderately oxidizing conditions, either acidic or alkaline (Vink, 1996).

Stibiconite occurs as yellow to dark yellow, fine-grained to dense aggregates replacing massive stibnite.

Pale pinkish to whitish pseudomorphs after flat sprays of stibnite on a sample with a matrix of realgar and stibnite turned to be not the expected Sb oxide, but quartz. Such pseudomorphs probably represent a replacement of stibnite by silica-rich late-hydrothermal solutions. In fact, Figure 44 in Antonović (1965) shows stibnite replaced by chalcedony.

Arsenolite (As_2O_3) was not observed as a direct oxidation product of realgar or other As-bearing primary phases. Arsenolite, which only occurs at extremely high activities of aqueous arsenic species (Vink, 1996), was observed, however, as a secondary phase in material of the tailings dump (Đorđević et al., 2018b).

Limonite is an uncommon oxidation product and was detected in very minor amounts in polished sections mainly. The observed trace elements (As, Sb, Si, S, Al, Ca and, rarely, P, Ni, Co and Cr, all in variable amounts), either structurally incorporated or adsorbed, reflect the mobilized element content of the primary ore minerals, the gangue minerals and the host rock(s). Co is derived from Co-bearing pyrite and vaesite, as well as from pentlandite and members of the thiospinel group.

Currently uncertain is the occurrence of triphuyite (?), $Fe^{3+}Sb^{5+}O_4$; the tentative identification is based on tiny bright (in BSE mode) grains within inconspicuous pale yellow crusts and spherulitic aggregates on a sample of partly weathered stibnite.

Carbonates

Two secondary carbonates, which are already briefly reported by Hiessleitner (1934), were found on the walls of narrow cracks in chromitite ore collected in the creek bed of the valley (approximate coordinates: 42.220516 N, 21.644152 E). Hydromagnesite, $Mg_5(CO_3)_4(OH)_2 \cdot 4H_2O$, a typical weathering product of serpentinite rocks, forms a thin white crust composed of tiny micaceous platelets with pearly lustre (Figure 6).

The PXRD pattern is in good agreement with a calculated powder pattern. Grown on the hydromagnesite crust is aragonite as tiny colourless, acicular glassy crystals (with pointed crystal terminations), which are partly intergrown in a spray-like arrangement.

Secondary magnesite, also reported in the early literature, is very rare as dull white, fine-grained nodular aggregates ("gel magnesite"). It is a characteristic alteration product of ultrabasic (serpentinite) rocks.

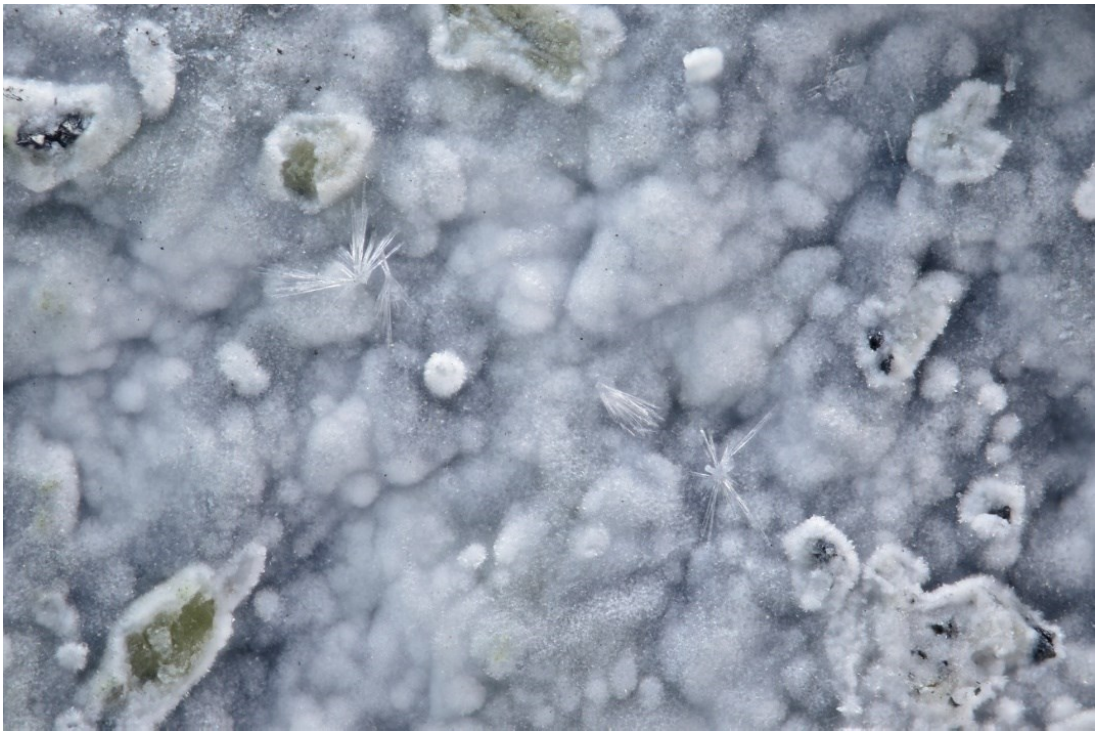

Fig. 6. Colour photo of grey-white, thin hydromagnesite crusts on serpentinite, which are overgrown by three very small sprays of acicular aragonite crystals. Field of view 3.5 mm. Collection Natural History Museum Vienna. Photo Harald Schillhammer

Sulphates

The most common secondary sulphate is gypsum. It forms colourless or off-white, lenticular crystals (partly with pseudorhombohedral habit) to prismatic individuals up to 5 mm in length, which sit on the surface of realgar-rich ore boulders or on the walls of thin cracks in such boulders. It is typically associated with the Mg arsenate hörnesite. Both have crystallizeds either contemporaneously or gypsum has formed later than hörnesite.In this paragenesis, gypsum also forms small rounded clusters composed of colourless glassy crystals, as well as distorted, partly skeletal individuals. Inconspicuous thin gypsum crusts are also relatively widespread on weathered ore-bearing samples.

Hexahydrite, $MgSO_4 \cdot 6H_2O$, was identified on a single specimen as white, thick, partly globular crusts with a fine-grained nature and dull lustre. Rozenite, $FeSO_4 \cdot 4H_2O$, forms white, very fine-grained and dull crusts and masses on aggregates of a partially weathered fine-grained iron sulphide (pyrite and/or marcasite) (Figure 7).

Locally, indistinct tiny curly rozenite aggregates are observed. Although rozenite was detected on only one sample so far, its very inconspicuous appearance suggests that it may be more common.

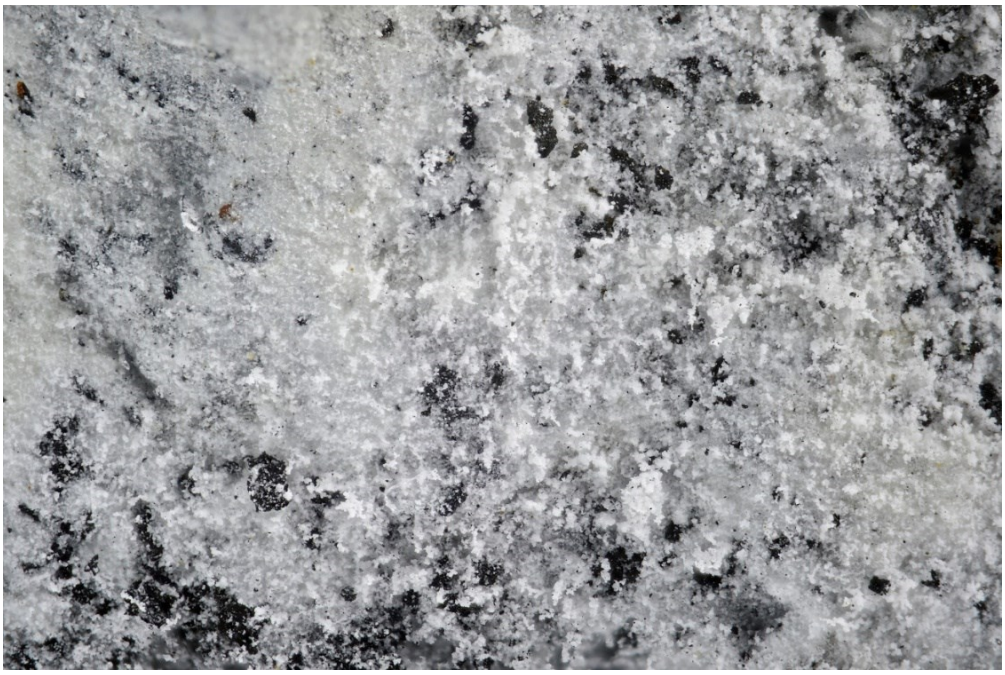

Fig. 7. Colour photo of the characteristically inconspicuous rozenite (white, very fine-grained crusts). Field of view 3.5 mm. Collection Natural History Museum Vienna. Photo Harald Schillhammer

Arsenates

The magnesium arsenate hörnesite, $Mg_3(AsO_4)_2 \cdot 8H_2O$, is, surprisingly, the most common secondary mineral and fairly widespread on and in weathered ore samples (Figure 8).

It preferably grows on the walls of thin cracks of realgar-rich ore boulders. Hörnesite appears as white radiating aggregates and spherulites (diameter up to 1.5 mm) of fibrous silky crystals, and also as thin white silky crust composed of chaotically arranged to radiating thin fibres (Figures 9 – 11).

Fig. 8. Crumbly efflorescences of white dullish hörnesite aggregates on the wall of the trench cutting the major dump. Photo T. Đ. in April 2018 (marker for scale)

Fig. 9. White sprays and radiating aggregates of hörnesite, associated with clusters of colourless, pseudo-rhombohedral gypsum crystals, both over growing red realgar (in top left partly altered to pararealgar). Colour photo, field of view 3.5 mm. Collection Natural History Museum Vienna. Photo Harald Schillhammer

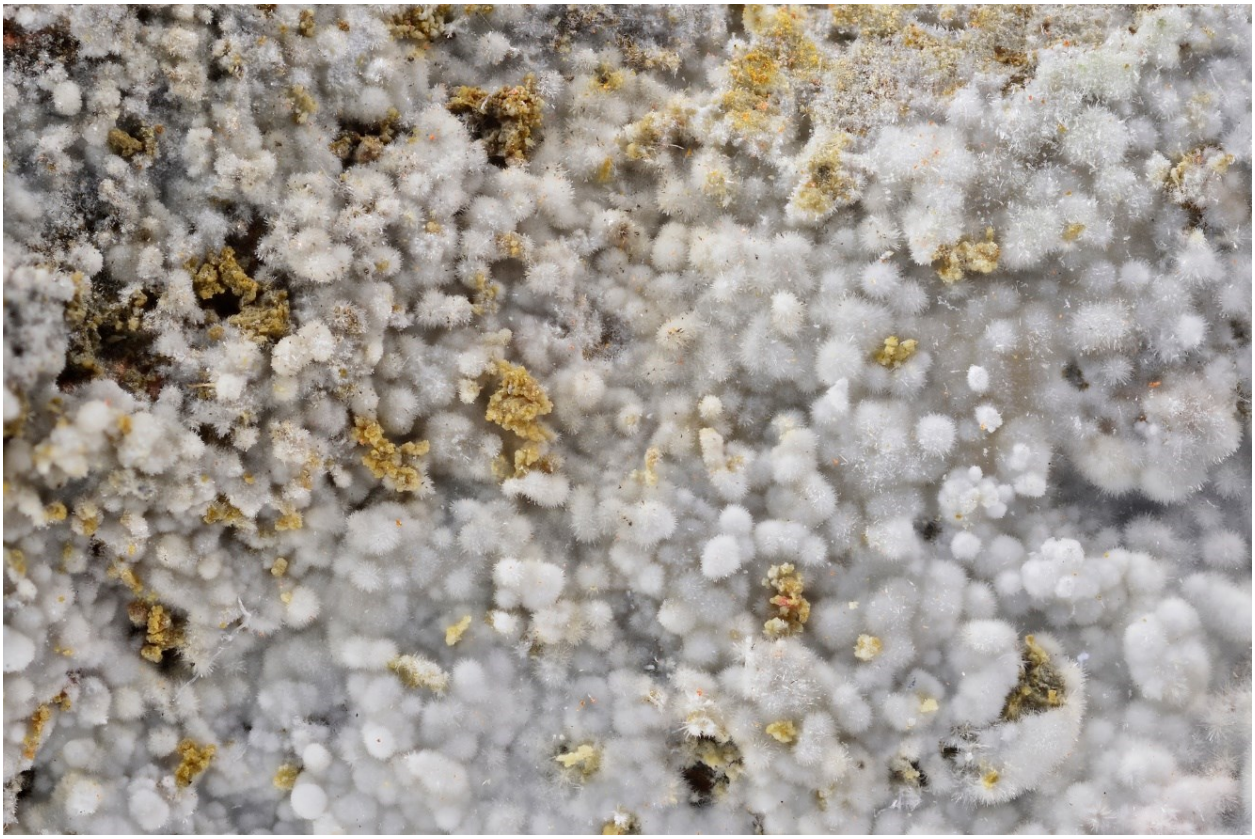

Fig. 10. White to pale grey coating of hörnesite, composed of radiating spherulitic aggregates. Colour photo, field of view 14 mm. Collection Natural History Museum Vienna. Photo Harald Schillhammer

Fig. 11. Loosely attached white hörnesite crusts composed of interlocking spherulitic aggregates built of radiating silky fibrous crystals. Colour photo, field of view 3.5 mm. Collection Natural History Museum Vienna. Photo Harald Schillhammer

Spherulitic aggregates can coat areas of up to 5 × 4 cm in size. A less aesthetic appearance show dull white globular aggregates, often crumbly, which appear to be hörnesite aggregates affected by percolating meteoric water in areas of the dump close to the surface. PXRD pattern of these dull aggregates reveal, however, no degradation of their crystallinity. Hörnesite is often accompanied by pseudo-rhombohedral, glassy crystals of gypsum. It appears that, once a very thin fissure has opened in a piece of realgar ore, percolating Mg-bearing meteoric water oxidizes and dissolves more realgar, leading to the crystallization of hörnesite.

Hörnesite was probably described as an unidentified mineral already by Hiessleitner (1951). He writes (translated from German): "*Next to secondary orpiment there is also a mineral that forms whitish, transparent, fibrous crystal crusts–arsenic –bearing? The oxidic efflorescent arsenic mineral arsenite or the Ca-hydrogenarsenate pharmacolite? – sample unfortunately was lost*."

We note that the "picropharmacolite" listed in the conference abstract of Đorđević et al. (2017), at that time only visually identified on two samples, turned out to be hörnesite. All other samples, which were on visual inspection very reminiscent of picropharmacolite, were also identified by PXRD as hörnesite. Pale greenish tints of a few hörnesite samples suggest that trace impurities of Ni may have been incorporated.

Annabergite, $Ni_3(AsO_4)_2 \cdot 8H_2O$, was detected as a very sparse component in polished sections. It fills interstitial voids in realgar (Figure 12) and appears to be rather a late-hydrothermal phase than a weathering product

Scorodite is uncommon and inconspicuous. The very stable iron arsenate, a widespread oxidation product of metal ore deposits (Drahota & Filippi, 2009; Majzlan et al., 2014), forms pale grey-green, partly globular, thin crustson drusy quartz coating thin fissures of a dark grey, cherty matrix (finely crystalline to massive quartz) containing fine-grained pyrite. Since no primary As minerals was visible under the optical microscope, a polished section of the specimen was investigated by SEM-EDS. This investigation revealed that the fine-grained pyrite (with grain sizes of ≤ 0.1 to 2 μm and rounded to cuboctahedral morphology) is the As source, since it almost always contains notable, albeit strongly variable amounts of As (up to S : As ~ 14) and Ni. The analytical data clear indicate an As-for-S substitution. Scorodite crusts on quartz were also encountered inside this polished section (Figure 13). Some spot analyses of the mineral showed trace amounts of S, Si and Sb.

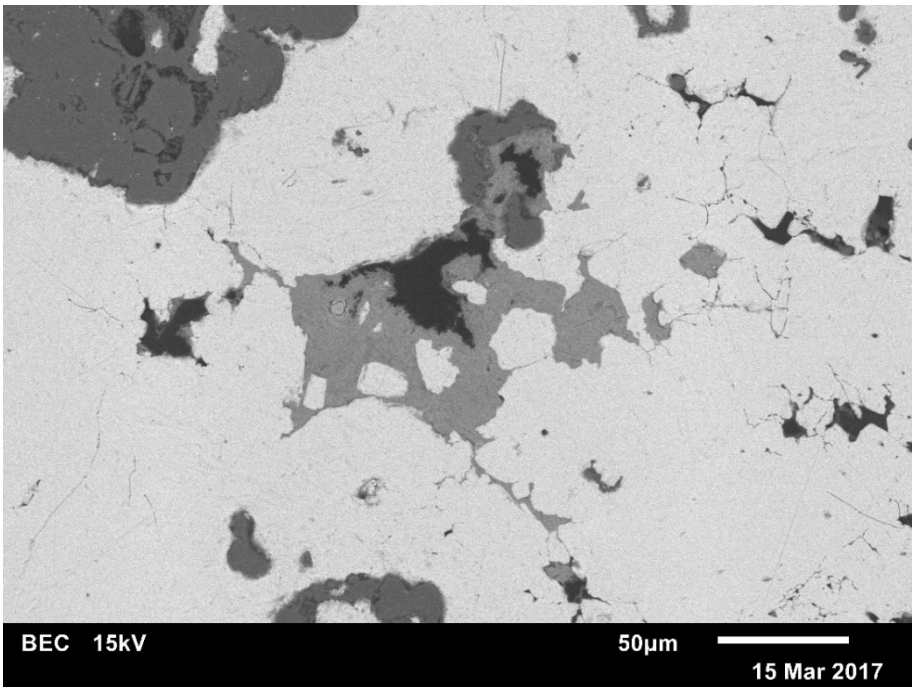

Fig. 12. SEM micrograph (BSE mode) showing more or less Mg-rich annabergite (grey in centre) filling interstitial voids in polycrystalline realgar (bright); minor quartz at top left (dark grey). Picture U. K.

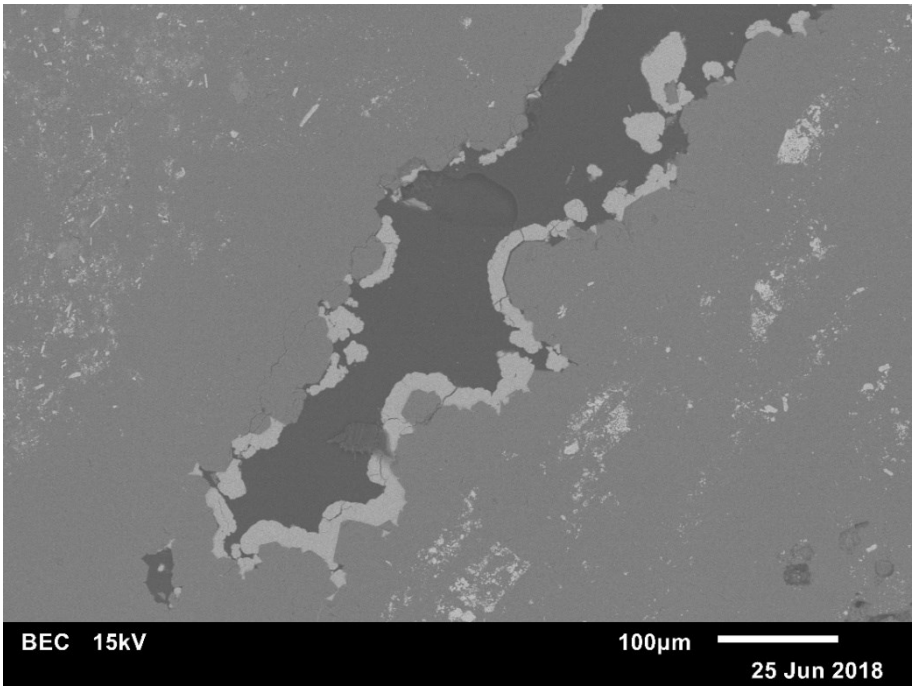

Fig. 13. SEM micrograph (BSE mode) showing thin, botryoidal to hemispherical scorodite crusts (bright grey) on quartz (grey); the dark grey material is resin. Picture U. K.

RAMAN SPECTRA

Raman spectra of hörnesite, hexahydrite and rozenite are shown in Figures 14–16. In general, these spectra are in good agreement with literature data (including the RRUFF database, rruff.info), although some of our spectra are of higher quality and cover a wider wave number range. For hörnesite a pronounced orientation effect is recognizable (Figure 14), explained by the distinct anisotropy of the crystal structure.

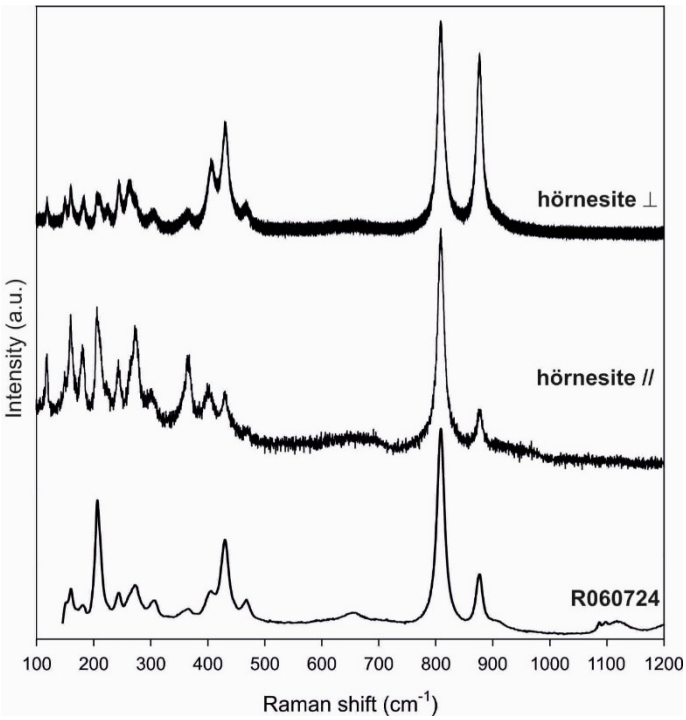

Fig. 14. Laser-Raman spectrum of hörnesite in two different orientations (perpendicular and parallel to elongation of acicular crystal), in comparison to spectrum of hörnesite sample R060724 from RRUFF database (rruff.org)

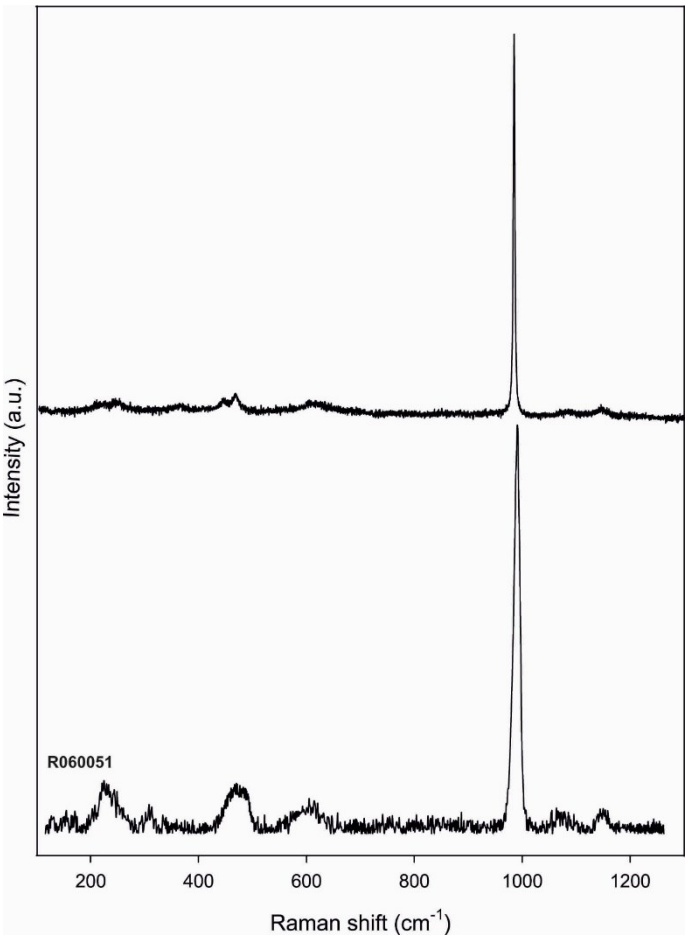

Fig. 15. Laser-Raman spectrum of randomly oriented hexahydrite in comparison to spectrum of hexahydrite sample R060051 from RRUFF database (rruff.org)

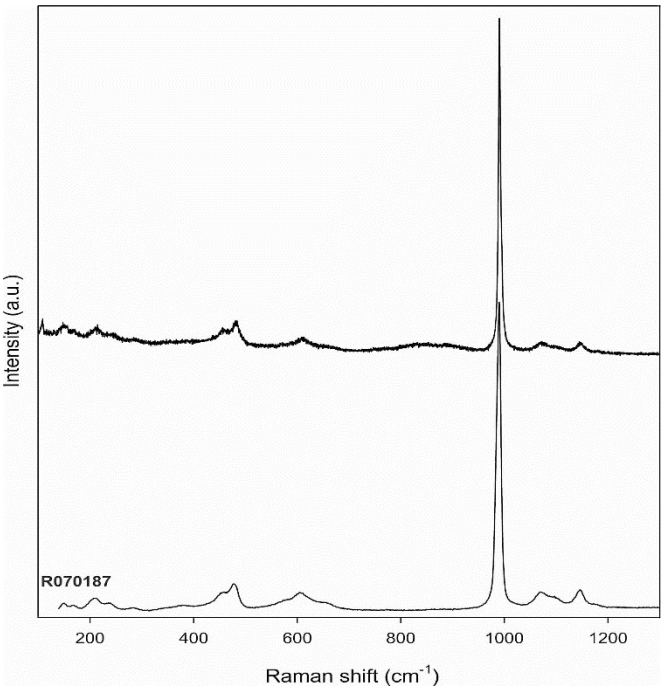

Fig. 16. Laser-Raman spectrum of randomly oriented rozenite in comparison to spectrum of rozenite sample R070187 from RRUFF database (rruff.org)

Measured hörnesite band positions and assignments are given in Table 3, where values are compared with literature values. In general, there is good agreement although the assignment of $\nu_2(AsO_4)$ and $\nu_4(AsO_4)$ bands by the different authors is contradictory.

For hexahydrite, a good agreement between measured band positions and assignments and positions listed in the literature is observed (Table 4).

As for rozenite, a comparison of measured band positions and assignments with those given in the literature is provided in Table 5. Again, good agreement is observed although some of the weak bands were not observed by all authors.

T a b l e 3

Raman band positions (wavenumbers in cm^{-1}) and band assignments for hörnesite, in comparison to literature values

Band positions				Band assignments
This work	Makreski et al. (2015)	Martens et al. (2004)	Frost et al. (2003b)	
117m, 150w, 161m, 181m, 210m, 224w, 244w, 273m	138w, 158m, 180vw, 205w, 242w, 262sh, 271m	147, 159, 181, 204, 209, 223, 242, 262, 273, 303, 308, 360, 366	117, 159, 180, 206, 218, 243, 262, 273, 303	Lattice vibrations
304w, 366w 366w(m)	301w, 365m	404, 430	363, 403 ("In-plane bends")	$\nu_2(AsO_4)$
408s (402w), 432s, 67m(w)	403w, 430m, 468vw	446, 467	429, 446, 467	$\nu_4(AsO_4)$
–	–	–	660	$\nu_{lib}(H_2O)$
810vs	808vs	808	807	$\nu_1(AsO_4)$
877vs(m)	875w	876	875, 907	$\nu_3(AsO_4)$
2890w, 3482w	–	2929, 3031, 3145, 3279, 3480	3030, 3166, 3479	$\nu_1(H_2O)$, $\nu_3(H_2O)$

Notes:
v = very, s = strong, m = medium, w = weak,br = broad, sh = shoulder.
Abbreviations: ν_1, symmetric stretching; ν_2, symmetric bending; ν_3, anti-symmetric stretching; ν_4, anti-symmetric bending; ν_{lib}, librational.
Raman spectra of hörnesite from a tailings dump are also given by Zhu et al. (2015), but no wavenumber values are listed.

T a b l e 4

Raman band positions (wavenumbers in cm^{-1}) and band assignments for hexahydrite, compared with literature values

Band positions			Band assignments
This work	Wang et al. (2006)*	Apopei et al. (2005)**	
203vw, 253vw, 351vw	223, 245, 364 (unassigned)	242vw, 370vw	Lattice vibrations
434w, 456w	445, 466	449sh, 469vw	$\nu_2(SO_4)$
611vw	610, (626)	611vw	$\nu_4(SO_4)$
982vs	983.6	985vs	$\nu_1(SO_4)$
1083vw, 1147vw,	(1079), (1088), 1085, 1146	1084vw, 1147vw	$\nu_3(SO_4)$
–	1655	1656vw	$\nu_2(H_2O)$
3264sh, 3416vw	3258, 3428	3268sh, 3398w	$\nu_1(H_2O)$, $\nu_3(H_2O)$

Notes:
v = very, s = strong, m = medium, w = weak,br = broad, sh = shoulder.
Abbreviations: ν_1, symmetric stretching; ν_2, symmetric bending; ν_3, anti-symmetric stretching; ν_4, anti-symmetric bending.
* "peak position values in parentheses were observed less commonly, possibly from crystal grains of different orientations" (Wang et al., 2006).
** No band assignments are given by Apopei et al. (2005).

T a b l e 5

Raman band positions (wavenumbers in cm^{-1}) and band assignments for rozenite, compared with literature values

Band positions		Band assignments
This work	Sharma et al. (2006), Chio et al. (2007)	
106m, 149w, 167w	94, 106, 148, 168	Lattice vibrations
212w, 234w, 243w, 286vw	211, 240, 286, 346, 382	$\nu_{trans}(Fe^{2+}, H_2O)$
458m, 480m	456, 480	$\nu_2(SO_4)$
610w	607, 622, 659	$\nu_4(SO_4)$
–	586, 784	$\nu_{lib}(H_2O)$
839vw, 895vw	–	$\nu_{1,3}(AsO_4)$?
991vs	990	$\nu_1(SO_4)$
1074vw, 1097sh, 1147vw	1071, 1096, 1146, 1176(?)	$\nu_3(SO_4)$
1594w, 1632vw	1590, 1629, 1679	$\nu_2(SO_4)$
–	3272(?)	$2\nu_2(SO_4)$
3411w	3334, 3376, 3438, 3533, 3593	$\nu_1(H_2O)$, $\nu_3(H_2O)$

Notes:
v = very, s = strong, m = medium, w = weak, br = broad, sh = shoulder.
Abbreviations: ν_1, symmetric stretching; ν_2, symmetric bending; ν_3, anti-symmetric stretching; ν_4, anti-symmetric bending; ν_{lib}, librational; ν_{trans}, translational.

DISCUSSION AND CONCLUSIONS

The conditions of formation of the supergene minerals at the Lojane deposit vary locally to a considerable extent, depending on the country rock matrix of the weathered ore samples. In general, oxidization of sulphides, sulpharsenides and arsenides in more or less wet conditions within ore

dumps and waste dumps, or on their surfaces produces sulphuric and arsenic acid, i.e. acidic conditions. However, in the presence of carbonate gangue (e.g. dolomite, calcite) and carbonate-bearing host rocks (e.g. limestone, dolostone, marble, serpentinite), which acts as a buffer to the acid water produced from the oxidation of the primary ore minerals, the resulting metal-bearing solutions will have a circumneutral or only slightly acidic pH. This is clearly the case in Lojane, where dolomite and calcite are gangue minerals and the host rock is a silicified serpentinite containing fine-grained, and therefore highly reactive, dolomite and, to a minor extent, magnesite. The strong tectonic fracturing of the serpentinite provided numerous pathways for weathering solutions. The dissolved arsenate originated from the weathering of the realgar and the magnesium derived from the alteration of the serpentinite have reacted to precipitate the most widespread arsenate at Lojane, hörnesite [$Mg_3(AsO_4)_2 \cdot 8H_2O$]. Hörnesite is a fairly stable arsenate hydrate mineral. In the system $CaO–MgO–As_2O_5–H_2O$ at 20°C, its synthetic counterpart represents the predominating phase (Stahl-Brasse & Guérin, 1971). Between temperatures of 0° and 100° no magnesium arsenates other than those with $8H_2O$ (= synthetic hörnesite) and $22H_2O$ (not known as a mineral) were obtained by synthesis from mixed solutions (de Schulten, 1903b). Hörnesite is stable up to ~100°C, where it loses the first part of its water molecules (De Schulten, 1903a,b, Frost et al., 2003a).

Hörnesite was observed to immobilize arsenic in anthropogenically modified geoenvironments. It was described as a secondary product of the reaction of Mg-rich ground waters with soils contaminated by As-bearing smelter wastes from California; soil pH at the contaminated site was measured to beabout 7.5 (Voigt et al., 1996). Hörnesite was also identified as a component of grey, weathered orpiment-realgar-bearing tailings at the Shimen carbonate-type realgar mine, China (Zhu et al., 2015). In these tailings, it is accompanied by the acid Ca arsenates pharmacolite and weilite (both dominant phases), and by the acid Ca-Mg arsenate picropharmacolite.

The strong pH buffering by the host rocks in Lojane explains that pharmacolite [$Ca(HAsO_4) \cdot 2H_2O$], a common acid arsenate and wide-spread alteration product of the weathering of As-rich ores (e.g. in Ste. Marie-aux-Mines, Vosges, France; Richelsdorf District, Hesse, Germany; Jáchymov, Czech Republic; Allchar, Macedonia; Lavrion, Greece; Bou Azzer, Morocco; for references see www.mindat.org) is not encountered in Lojane. Similarly, two other common acid arsenates, picropharmacolite [$Ca_4Mg(AsO_4)_2(HAsO_4)_2 \cdot 11H_2O$] and weilite [Ca(HAsO4)], were also not detected. Furthermore, acid magnesium arsenates such as brassite [$Mg(HAsO_4) \cdot 4H_2O$] and roesslerite [$Mg(HAsO_4) \cdot 4H_2O$] were as well not observed as weathering products.

The non-acid pH values of the weathering solutions promote oxidation since it was shown repeatedly that the oxidation rates of arsenic sulphides (orpiment and realgar or their amorphous analogues) increase with increasing pH values at ambient conditions (Lengke & Tempel, 2002, 2003, 2005, 2009).

In iron-rich weathering environments, arsenate anions are strongly adsorbed on ferric iron oxyhydroxide phases ("limonite", goethite, ferrihydrite, amorphous materials) resulting in a stop to the spreading of arsenate into the environment. However, at high concentrations of bicarbonate and carbonate, As can be released from Fe oxyhydroxide surfaces back to the solution because of surface charge, or may also act as a competitor for both As^{5+} and As^{3+} during sorption reactions (Lengke & Tempel, 2009). Lojane is unusual in that ferric iron oxyhydroxide phases are very rare as weathering products. Thus, the retention of arsenate does not happen and only the precipitation of the arsenate as hörnesite precludes its further migration into the environment.

If the matrix is cherty, as is the case of Lojane samples containing disseminated fine-grained pyrite (generally Ni^- and/or As-bearing), vaesite and/or pyrrhotite, the oxidation of the Fe sulphides produces low-pH solutions as there is no buffering by carbonates. Under such conditions, the observed Fe arsenate scorodite and the Fe sulphate rozenite will crystallize. If primary Fe sulphide weathers in a Mg-rich serpentinite environment, the Mg sulphate hexahydrite will form. Considering the temperature- and humidity-dependent equilibrium between hexahydrite, $MgSO_4 \cdot 6H_2O$, and the higher hydrate epsomite, $MgSO_4 \cdot 7H_2O$ (Chou & Seal, 2003), as well as the dehydration cracks observed in the globular, fine-grained hexahydrite aggregates, it seems probable that hexahydrite formed in the dump as a dehydration product of epsomite at temperatures higher than about 40 – 60 °C, depending on seasonal humidity.

It seems surprising that jarosite [$KFe_3(SO_4)_2(OH)_6$], normally a very common oxidation product in iron(III)- and sulphate-rich acid environments, has not been detected yet among the secondary

phases. Neither found was its hydronium analogue hydroniumjarosite. A probable explanation is that both the pH-buffering Mg-rich environment (serpentinite hosting the As-Sb sulphide mineralization) and the only very minor amounts of primary K minerals (phlogopite in serpentinite; muscovite and K-feldspar in areas affected by the granitoid and rhyolite intrusions), are unfavorable for jarosite crystallization. Nonetheless, the mineral might be detected in microenvironments.

The behaviour of antimony during weathering of stibnite, the ore mineral mined at Lojane, is quite different from that of the toxic arsenic. Unlike the later, antimony is a potentially toxic trace element with no known biological function (Shotyk et al., 2005). Sb(III) is more toxic than Sb(V) (Winship, 1987; Sundar & Chakravarty, 2010). Antimony(V) is also adsorbed on ferric iron oxyhydroxides, but much less so than arsenic. The situation at Lojane is similar to that at a historic antimony mine in New Zealand where negligible attenuation of the metalloids Sb and As (from arsenopyrite) occurred via adsorption outside the adit, as iron oxyhydroxide is rare at the New Zealand mine site. We observed that, at Lojane, Sb is not very mobile by comparison with As. This agrees well with literature data (e.g. Fawcett & Jamieson, 2011; Fawcett et al., 2015).

Belzile et al. (2001) reported that oxidation of Sb(III) to Sb(V) by amorphous Fe and Mn oxyhydroxides in sediments and natural waters is always rapid. Since Fe oxyhydroxides are rare in Lojane and Mn oxyhydroxides nearly non-existent, Sb(III) prevails in Lojane, in the form of Sb_2O_3 (valentinite and senarmontite), although strongly weathered stibnite ore was partly transformed into "stibiconite", a mixed Sb(III)-Sb(V) oxyhydroxide. The mixed Sb(III)-Sb(V) oxides cervantite and clinocervantite, both $Sb^{3+}Sb^{5+}O_4$, were not detectable, but are expected to be present. The Fe(III)-Sb(V) oxide tripuhyite was not reliably confirmed so far.Tripuhyite was recently recognized as a very common Sb-bearing secondary phase in Fe-As-Sb mine wastes and soils at several Sb deposits in Slovakia (Lalinská et al., 2017).

The mobilization of nickel during oxidation of primary Ni or Ni-bearing minerals (predominantly vaesite, Ni-bearing pyrite and gersdorffite, but also subordinate to trace pentlandite, violarite and millerite) is reflected in the appearance of very minor amounts of annabergite, $Ni_3(AsO_4)_2 \cdot 8H_2O$, and Ni-bearing roméite-group minerals. Trace amounts of Ni may also be present in hörnesite (and hexahydrite?), as suggested a very pale greenish tint of some white globular efflorescences, but this has not been investigated yet. Geochemical studies of soils and sediments around the Lojane As-Sb mine showed Ni contents of up to 1119 mg kg^{-1} (median value: 322 mg kg^{-1}) (Alderton et al., 2014).

Finally, the present study indicates only negligible mobilization of Cr by weathering processes. Although anhedral grains of chromite and magnesiochromite are often encountered within serpentine, sulphide-bearing chert and massive realgar-stibnite ore, neither rims of any secondary Cr minerals formed around these grains, nor was Cr observed as an impurity elements in other secondary phases, except in rare limonite (thin weathering coating around pentlandite grain) and in scorodite crusts.These observations are in agreement with literature data on weathered Cr deposits (Garnier et al., 2008) and are explained by the extreme stability of the chromite and magnesiochromite. Nonetheless, it is known that trace amounts of Cr can be leached by natural processes from serpentinite bedrock and transported as Cr^{6+} species in ground water (Godgul & Sahu, 1995; Steinpress, 2005; Moraki, 2010) as well as from a chromite mine overburden (Dhal et al., 2013).In soils and sediments around the Lojane As-Sb mine, Cr contents of up to 595 mg kg^{-1} were measured, with a median value of 285 mg kg^{-1} (Alderton et al., 2014; Tasev et al., 2017). Measurements of Cr(aq) contents in ground water are not available yet.

Acknowledgements: We acknowledge the financial support of the Federal Ministry of Science, Research and Economy, Program Scientific & Technological Cooperation between Macedonia and Austria 2016–2018 (MK 05/2016) and of the Austrian Science Fund (FWF) (P 30900-N28).We thank Goran Batic (Natural History Museum Vienna) for the careful preparation of the polished sections.The article benefited from helpful comments by Vlado Bermanec.

REFERENCES

[1] Alderton, D., Serafimovski, T., Burns, L., Tasev, G. (2014): Distribution and mobility of arsenic and antimony at mine sites in FYR Macedonia. *Carpathian Journal of Earth and Environmental Sciences*, **9**, 43–56.

[2] Antonović, A., Deleon, G., Divjan, S., Radusinović, D. (1957): The Lojane complex ores (As, Sb, Ni, Co). *Second Geol. Congr. Yugoslavia*, 494–503 (in Serbian).

[3] Antonović, A. (1965): Geology, tectonic structure and genesis of the arsenic-antimony ore deposits in the Lojane and

Nikuštak district (Skopska Crna Gora Mts). *Geological Institute, Skopje, Special Issue no*. **1**, 77 pp. (in Macedonian).

[4] Apopei, A. I., Buzgar, N., Damian, G., Buzatu, A. (2005): The Raman study of weathering minerals from the Coranda-Hondol open pit (Certej gold-silver deposit) and their photochemical degradation products under laser irradiation. *Canadian Mineralogist*, **52**, 1027–1038.

[5] Ashley, P. M., Craw, D., Graham, B. P., Chappell, D. A. (2003): Environmental mobility of antimony around mesothermal stibnite deposits, New South Wales, Australia, and southern New Zealand. *Journal of Geochemical Exploration*, **77**, 1–14.

[6] Augé, T., Morin, G., Bailly, L., Serafimovsky, T. (2017): Platinum-group minerals and their host chromitites in Macedonian ophiolites. *European Journal of Mineralogy*, **29**, 585–596.

[7] Belzile, N., Chen, Y. W., Wang, Z. J. (2001): Oxidation of antimony(III) by amorphous iron and manganese oxyhydroxides. *Chemical Geology*, **174**, 379–387.

[8] Chio, C. H., Sharma, S. K., Muenow, D. W. (2007): The hydrates and deuterates of ferrous sulfate ($FeSO_4$): a Raman spectroscopic study. *Journal of Raman Spectroscopy*, **38**, 87–99.

[9] Chou, I-M. & Seal II, R. R. (2003): Determination of epsomite–hexahydrite equilibria by the humidity-buffer technique at 0.1 MPa with implications for phase equilibria in the system $MgSO_4$-H_2O. *Astrobiology*, **3**, 619–630.

[10] De Schulten, A. (1903a): About peculiar characteristics of some salt hydrates. *Bulletin de la Société Chimique de France*, **29**, 724–726 (in French).

[11] de Schulten, A. (1903b): Crystallised magnesium phosphate and arsenate: artificial production of bobierrite and hoernesite. *Bulletin de la Société Française de Minéralogie*,**26**, 81–86 (in French).

[12] Deleon, G. (1959): Structural characteristics of arsenic-antimony ore from the Lojane mine. *Glasnik Prirod. muzeia u Beogradu, Ser. A*, **11**, 109–114.

[13] DeSisto, S. L., Jamieson, H. E., Parsons, M. B. (2016): Subsurface variations in arsenic mineralogy and geochemistry following long-term weathering of gold mine tailings. *Applied Geochemistry*, **73**, 81–97.

[14] Dhal, B., Das, N. N., Thatoi, H. N., Pandey, B. D. (2013): Characterizing toxic Cr(VI) contamination in chromite mine overburden dump and its bacterial remediation. *Journal of Hazardous Materials*, **260**, 141–149.

[15] Diemar, G. A., Filella, M., Leverett, P., Williams, P. A. (2009): Dispersion of antimony from oxidizing ore deposits. *Pure and Applied Chemistry*, **81**, 1547–1553.

[16] Đorđević, T., Kolitsch, U., Tasev, G., Serafimovski, T., Boev, B. (2017): Anomalous As-enrichment in gersdorffite in a realgar-rich environment: Lojane, Macedonia. *Mitteilungen der Österreichischen Mineralogischen Gesellschaft*, **163**, p. 38 (abs.).

[17] Đorđević, T., Kolitsch, U., Tasev, G., Serafimovski, T. (2018a): First insights into the mineralogy of the tailings dump of the Lojane Sb-As(-Cr) deposit, FYR of Macedonia. *Geophysical Research Abstracts*, **20**, 14914 (abs.).

[18] Đorđević, T., Kolitsch, U., Serafimovski, T., Tasev, G., Tepe, N., Stöger-Pollach, M., Hofmann, T., Boev. B. (2018b): Mineralogy and supergene weathering of the realgar-rich flotation tailings at the former As-Sb-Cr mine of Lojane, FYR of Macedonia. *Canadian Mineralogist* (to be submitted).

[19] Drahota, P. & Filippi, M. (2009): Secondary arsenic minerals in the environment: A review. *Environment International*, **35**, 1243–1255.

[20] Fawcett, S. E. & Jamieson, H. E. (2011): The distinction between ore processing and post-depositional transformation on the speciation of arsenic and antimony in mine waste and sediment. *Chemical Geology*, **283**, 109–118.

[21] Fawcett, S. E., Jamieson, H. E., Nordstrom, D. K., McCleskey R. B. (2015): Arsenic and antimony geochemistry of mine wastes, associated waters and sediments at the Giant Mine, Yellowknife, Northwest Territories, Canada. *Applied Geochemisty*, **62**, 3–17.

[22] Frost, R. L., Weier, M. L., Martens, W., Kloprogge, J. T., Ding, Z. (2003a): Thermal decomposition of the vivianite arsenates – implications for soil remediation. *Thermochimica Acta*, **403**, 237–249.

[23] Frost, R. L., Martens, W., Williams, P. A., Kloprogge, J. T. (2003b): Raman spectroscopic study of the vivianite arsenate minerals. *Journal of Raman Spectroscopy*, **34**, 751–759.

[24] Garnier, J., Quantin, C., Guimarães, E., Becquer, T. (2008): Can chromite weathering be a source of Cr in soils? *Mineralogical Magazine*, **72**, 49–53.

[25] Godgul, G. & Sahu, K. C. (1995): Chromium contamination from chromite mine. *Environmental Geology*, **25**, 251–257.

[26] Grafenauer, S. (1977): Genesis of chromite in Yugoslavian peridotite. In: Klemm, D.D. & Schneider, H.-J. (Eds.): *Time- and Strata-Bound Ore Deposits*. Springer, pp. 327–351.

[27] Hiessleitner, G. (1931): Geologie mazedonischer Chromeisenlagerstätten. *Berg- und Hüttenmännisches Jahrbuch der Montanistischen Hochschule in Leoben*, **79**, 47–57 (in German).

[28] Hiessleitner, G. (1934): Einbruch von Granit und Andesit in Chromerze führenden Serpentin von Lojane, NNW Kumanovo in Südserbien. *Zeitschrift für Praktische Geologie*, **42**, 81–88 (in German).

[29] Hiessleitner, G. (1951): Serpentin- und Chromerzgeologie der Balkanhalbinsel und eines Teiles von Kleinasien. *Jahrbuch der Geologischen Bundesanstalt, Sonderband* **1**, 1–255 (in German).

[30] Janković, S. (1989): Sb-As-Tl mineral associations in the Mediterranean region. *International Geology Review*, **31**, 262–273.

[31] Japan International Cooperation Agency (JICA), Ministry of Agriculture, Forestry and Water Economy (MAFWE), The Former Yugoslav Republic of Macedonia (2008): The study on capacity development for soil contamination management related to mining in the Former Yugoslav Republic of Macedonia. Final Report, Vol. **II**, Main Report, March 2008, Mitsubishi Materials Natural Resources Development Corporation, 159 pp. [http://open_jicareport.jica.go.jp/pdf/11900271_01.pdf]

[32] Jovanovski, G., Makreski, P., Kaitner, B., Šoptrajanov, B. (2009): Minerals from Macedonia. X-ray powder diffraction *vs*. vibrational spectroscopy in mineral identification. *Contributions, Sec. Math. Tech. Sci., MANU*, **XXX** (1–2), 7–34.

[33] Karamata, S. (1983): Contents of some microelements in the Tertiary magmatites of eastern part of Yugoslavia related to their geotectonic position. *Glas SANU*, CCVXXXV, Department of Natural and Mathematical Sciences, 49, 39–54 (in Serbian).

[34] Lalinská, B., Majzlan, J., Klimko, T., Chovan, M., Kučerová, G., Michňová, J., Hovorič, R., Göttlicher, J., Steininger, R (2012): Mineralogy of weathering products of Fe-As-Sb mine wastes and soils at several Sb deposits in Slovakia. *Canadian Mineralogist*, **50**, 481–500.

[35] Lengke, M. F. & Tempel, R. N. (2002): Reaction rates of natural orpiment oxidation at 25 to 40°C and pH 6.8 to 8.2 and comparison with amorphous As_2S_3 oxidation. *Geochimica et Cosmochimica Acta*, **66**, 3281–3291.

[36] Lengke, M. F. & Tempel, R. N. (2003): Natural realgar and amorphous AsS oxidation kinetics. *Geochimica et Cosmochimica Acta*, **67**, 859–871.

[37] Lengke, M. F. & Tempel, R. N. (2005): Geochemical modeling of arsenic sulfide oxidation kinetics in a mining environment. *Geochimica et Cosmochimica Acta*, **69**, 341–356.

[38] Lengke, M. F., Sanpawanitchakit, C., Tempel, R. N. (2009): The oxidation and dissolution of arsenic-bearing sulfides. *Canadian Mineralogist*, **47**, 593–613.

[39] Lu, P. & Zhu, C. (2011): Arsenic Eh–pH diagrams at 25°C and 1 bar. *Environmental Earth Sciences*, **62**, 1673–1683.

[40] Majzlan, J., Drahota, P., Filippi, M. (2014): Parageneses and crystal chemistry of arsenate minerals. *Reviews in Mineralogy and Geochemistry*, **79**, 17–184.

[41] Makreski, P., Stefov, S., Pejov, Lj., Jovanovski, G. (2015): Theoretical and experimental study of the vibrational spectra of (para)symplesite and hörnesite. *Spectrochimica Acta A*, **144**, 155–162.

[42] Martens, W. N., Kloprogge, J. T., Frost, R. L., Rintoul, L. (2004): Single-crystal Raman study of erythrite, $Co_3(AsO_4)_2 \cdot 8H_2O$. *Journal of Raman Spectroscopy*, **35**, 208–216.

[43] Meixner, H. (1949): Einige interessante Mineralfunde (Vesuvian, Apophyllit) aus dem Serpentingebiet von Lojane in Südserbien. *Neues Jahrbuch für Mineralogie, Geologie und Paläontologie, Abhandlungen, Abteilung A: Mineralogie, Petrographie*, **1949** (1–3), 73–77 (in German).

[45] Moraki, A. (2010): Assessment of groundwater contamination by hexavalent chromium and its remediation at Avlida area, Central Greece. *Hellenic Journal of Geosciences*, **45**, 175–184.

[46] Mudrinić, Č. (1978): *Geochemical features of Sb-As associations within the Serbo-Macedonian metallogenic province*. PhD Thesis, Faculty of Mining and Geology, Belgrade, 125 pp. (in Serbian).

[47] Palache, C., Berman, C., Frondel, C. (1951): *Dana's System of Mineralogy*. 7th ed., Vol. **II**. John Wiley, New York, 1124 pp. (p. 264).

[48] Pamić, J. (2002): The Sava-Vardar Zone of the Dinarides and Hellenides versus the Vardar Ocean. *Eclogae geologicae Helvetiae*, **95**, 99–113.

[49] Panikorovskii, T. L., Shilovskikh, V. V., Avdontseva, E. Yu., Zolotarev, A. A., Karpenko, V. Y., Mazur, A. S., Yakovenchuk, V. N., Bazai, A. V., Krivovichev, S. V., Pekov, I. V. (2017): Magnesiovesuvianite, $Ca_{19}Mg(Al,Mg)_{12}Si_8O_{69}(OH)_9$, a new vesuvianite-group mineral. *Journal of Geosciences*, **62**, 25–36.

[50] Radusinović, D. R. (1966): Greigite from the Lojane chromium deposit, Macedonia. *American Mineralogist*, **51**, 209–215.

[51] Roper, A. J., Williams, P. A., Filella, M. (2012): Secondary antimony minerals: Phases that control the dispersion of antimony in the supergene zone. *Chemie der Erde-Geochemistry*, **72**, Supplement **4**, 9–14.

[52] Serafimovski, T. (1990): *Metalogeny of the zone Lece-Chalkidiki*. Doctoral thesis, Faculty of Mining and Geology, University "Goce Delčev" – Štip, Štip, Macedonia, 380 pp. (in Macedonian).

[53] Serafimovski, T. (1993): *Structural-metallogenic features of the Lece-Chalkidiki zone: Types of mineral deposit and distribution*. Faculty of Mining, University "Goce Delčev" – Štip, Štip, Macedonia, Special Issue no. **2**, 325 pp.

[54] Schumacher, F. (1954): The ore deposits of Yugoslavia and the development of its mining industry. *Economic Geology*, **49**, 451–492.

[55] Sharma, S. K., Chio, C. H., Muenow, D. W. (2006): Raman spectroscopic investigation of ferrous sulfate hydrates. *Lunar and Planetary Science*, XXXVII, Houston, Texas, USA, 1078.pdf.

[56] Shotyk, W., Krachler, M., Chen, B. (2005): Anthropogenic impacts on the biogeochemistry and cycling of antimony. *Metal Ions in Biological Systems*, **44**, 171–203.

[57] Steinpress, M. G. (2005): Naturally occurring chromium(VI) in groundwater, including the Presidio of San Francisco case study. In: Guertin, J., Jacobs, J. A., Avakian, C. P. (Eds.), *Chromium(VI) Handbook*, 94–137.

[58] Stuhlberger, C. (Ed.) (2010): *Mining and Environment in the Western Balkans*. ENVSEC, 108 pp. [http://www.unep.org/pdf/MiningBalkans_screen.pdf]

[59] Sundar, S. & Chakravarty, J. (2010): Antimony toxicity. *International Journal of Environmental Research and Public Health*, **7**, 4267–4277.

[60] Tajder, M. (1938): Nemalite from Lojane (Serbia). *Vesnik Geol. Inst. Jugoslavije*, **6**, 239–240 (in Croatian/German).

[61] Tajder, M. (1939): Green hornblende, asbestos, phlogopite, zircon and apatite from Lojane near Kumanovo. *Neues Jahrbuch für Mineralogie, Geologie und Paläontologie, Abhandlungen, Abteilung A: Mineralogie, Petrographie*, **1939**, Ref. **I**, 135–136.

[62] Tasev, G., Serafimovski, T., Djordjević, T., Boev, B. (2017): Soil and groundwater contamination around the Lojane As-Sb mine, Republic of Macedonia. *17th International Multidisciplinary Scientific Geoconference SGEM2017, 29 June – 5 July, Albena, Bulgaria, Conference Proceedings*, **17**, 809–817.

[63] United Nations Environment Progamme (UNEP) (2000): *Post-Conflict Environmental Assessment – FYR of Macedonia*. UNEP, Geneva, Switzerland, 88 pp. [https:// postconflict.unep.ch/publications/fyromfinalasses.pdf]

[64] Vink, B.W. (1996): Stability relations of antimony and arsenic compounds in the light of revised and extended Eh–pH diagrams. *Chemical Geology*, **130**, 21–30.

[65] Voigt, D. E., Brantley, S. L., Hennet, R. J. C. (1996): Chemical fixation of arsenic in contaminated soils. *Applied Geochemistry*, **11**, 633–643.

[66] Vujanović, V. (1958): Ein ungewöhnliches Erzvorkommen bei Nikuštak (Makedonien). *Neues Jahrbuch für Mineralogie, Monatshefte*, **1958**, 106–113.

[67] Wang, A., Freeman, J. F., Jolliff, B. L., Chou, I-M. (2006): Sulfates on Mars: A systematic Raman spectroscopic study of hydration states of magnesium sulfates. *Geochimica et Cosmochimica Acta*, **70**, 6118–6135.

[68] Williams, S. & Marstijepovic, S. (2010): Western Balkans Environmental Program. Case Studies on Remediation of Environmental Hot Spots in the Western Balkans. *UNDP Montenegro*, 176 pp. [http://westernbalkansenvironment.net/documents/case_studies.pdf]

[69] Wilson, N. J., Craw, D., Hunter, K. (2004): Contributions of discharges from a historic antimony mine to metalloid content of river waters, Marlborough, New Zealand. *Journal of Geochemical Exploration*, **84**, 127–139.

[70] Winship, K. A. (1987): Toxicity of antimony and its compounds. *Adverse Drug Reactions and Acute Poisoning Reviews*, **6**, 67–90.

[71] Zhu, X., Wang, R., Lu, X., Liu, H., Li, J., Ouyang, B., Lu, J. (2015): Secondary minerals of weathered orpiment-realgar-bearing tailings in Shimen carbonate-type realgar mine, Changde, Central China. *Mineralogy and Petrology*, **109**, 1–15.

Р е з и м е

СУПЕРГЕНА МИНЕРАЛОГИЈА НА НАОЃАЛИШТЕТО НА Sb-As-Cr ЛОЈАНЕ, РЕПУБЛИКА МАКЕДОНИЈА: СЛЕДЕЊЕ НА МОБИЛИЗАЦИЈАТА НА ТОКСИЧНИТЕ МЕТАЛИ

Уве Колич[1,2], Тамара Ѓорѓевиќ[2], Горан Тасев[3], Тодор Серафимовски[3], Иван Боев[3], Блажо Боев[3]

[1]Оддел за минералогија и петрографија, Природно-историски музеј, Бургринг 7, А-1010 Виена, Австрија;
[2]Институт за минералогија и кристалографија, Универзитет во Виена, Алтанштрасе. 14, А-1090 Виена, Австрија
[3]Факултет за природно-технички науки, Универзитет "Гоце Делчев" во Штип, Гоце Делчев 89, 2000 Штип, Р. Македонија
uwe.kolitsch@nhm-wien.ac.at

Клучни зборови: наоѓалиште Лојане; Република Македонија; супергена минералогија; арсен; антимон; хром

Како дел од еден поголем проект од аспект на животната средина за минералогијата и геохемијата на наоѓалиштето на Sb-As-Cr Лојане, Република Македонија, кое било експлоатирано за хромит, а подоцна и за стибнит сè до 1979 година, а е и значителен извор на загадување со арсен и антимон, беше проучувана супергената минералогија на наоѓалиштето. Беа земени примероци од руда и јаловински материјал заради одредба и карактеризирање на претходно неистражени пакети на супергени минерални фази со помош на стандардни минералошки техники. Беа одредени следните видови (по абецеден ред): анабергит, арсеносидерит(?), гипс, хексахидрит, хернезит, парареалгар, минерали од ромеитската група, розенит, скородит, сенармонтит, стибиконит, сулфур, трипухит и валентинит. Опишан е начинот на нивното појавување и се дискутираат услови на нивното локално формирање. Дадени се раманските спектри со висока резолуција на хорнезит, хексахидрит и розенит и споредени се со податоците од литературата. Mg-арсенатхорнесит е далеку најчестиот секундарен арсенат (и имобилизатор на арсен), карактеристика што ѝ се припишува на серпентинитската матрица богата со Mg и карбонат, која ги неутрализира сите кисели алтерациски раствори. Антимонот е ефикасно имобилизиран во секундарните Sb(III) оксиди, но количини во траги исто така се вклучени во скородитот. Никелот, кој потекнува од примарни никлоносни сулфидни и сулфарсенидни минерали, е мобилизиран и инкорпориран во анабергитот и хемиски променливите минерали од ромеитската група. Не е забележана мобилизација на Cr, што е во согласност со литературните податоци распаднати наоѓалишта на Cr.